Research Paper
J. Astron. Space Sci. 31(4), 303-309 (2014)
http://dx.doi.org/10.5140/JASS.2014.31.4.303

JASS Journal of Astronomy and Space Sciences

Prediction Model of the Outer Radiation Belt Developed by Chungbuk National University

Dae-Kyu Shin, Dae-Young Lee†, Jin-Hee Kim, Jung-Hee Cho
Department of Astronomy and Space Science Chungbuk National University Cheongju 361-763, Korea

The Earth's outer radiation belt often suffers from drastic changes in the electron fluxes. Since the electrons can be a potential threat to satellites, efforts have long been made to model and predict electron flux variations. In this paper, we describe a prediction model for the outer belt electrons that we have recently developed at Chungbuk National University. The model is based on a one-dimensional radial diffusion equation with observationally determined specifications of a few major ingredients in the following way. First, the boundary condition of the outer edge of the outer belt is specified by empirical functions that we determine using the THEMIS satellite observations of energetic electrons near the boundary. Second, the plasmapause locations are specified by empirical functions that we determine using the electron density data of THEMIS. Third, the model incorporates the local acceleration effect by chorus waves into the one-dimensional radial diffusion equation. We determine this chorus acceleration effect by first obtaining an empirical formula of chorus intensity as a function of drift shell parameter L^*, incorporating it as a source term in the one-dimensional diffusion equation, and lastly calibrating the term to best agree with observations of a certain interval. We present a comparison of the model run results with and without the chorus acceleration effect, demonstrating that the chorus effect has been incorporated into the model to a reasonable degree.

Keywords: energetic electrons, radiation belts, wave-particle interaction

1. INTRODUCTION

The Earth is surrounded by two well-known radiation belts, the inner and outer belts, both containing high energy charged particles. The two belts are separated by the slot region. The inner belt is relatively stable, and the outer belt suffers from substantial changes due to various reasons (e.g., Kim et al. 2011, Lee et al. 2013). The outer belt variations include the long-term solar cycle-dependent variation (Li et al. 2011, Lee et al. 2013), an immediate response on a minute time scale when the magnetosphere is directly hit by solar wind shock (Li et al. 1993), and the more usual variations on an intermediate time scale, typically hours to days. The currently prevailing view for the physical reason responsible for such variations is largely, though not necessarily exclusively, based on the global transport and the more local wave-particle interaction. The observed flux at a given time and location by a satellite is a net result of delicate balance between the acceleration (source) and loss effects (Reeves et al. 2003).

The plasma sheet supplies the seed electrons and ions particularly under the enhanced convection, substom and storm times. The transported electrons themselves become the radiation belt components after acceleration by plasma waves as well as by radial diffusion process. The most responsible plasma wave for acceleration is believed to be whistler chorus usually identified outside the plasmasphere (Horne & Thorne 2003). The chorus waves can also act to scatter electrons to precipitate into the upper atmosphere (Horne & Thorne 2003, Lam et al. 2010). Other waves such as electromagnetic ion cyclotron waves and plasmaspheric hiss waves can also contribute to atmospheric loss (Summers & Meredithet al. 2007 Kim

Received Oct 21, 2014 **Revised** Nov 15, 2014 **Accepted** Nov 20, 2014
†**Corresponding Author**
E-mail: dylee@chungbuk.ac.kr, ORCID: 0000-0001-9994-7277
Tel: +82-43-261-2316, Fax: +82-43-274-2312

http://janss.kr pISSN: 2093-5587 eISSN: 2093-1409

et al. 2011). The electrons can also be lost into the solar wind through magnetopause crossing under stressed condition by solar wind (Kim et al. 2008, 2010, Turner et al. 2012, Hwang et al. 2013). The electron flux dropout has also been attributed to magnetic field line stretching (Onsager et al. 2002, Lee et al. 2006).

Quantitative specification of all these effects is the main trend of the present day research in this field. On one side, observations by satellites such as CRRES (e.g., Meredith et al. 2000) and more recent Van Allen Probes (e.g., Baker et al. 2013) have improved our understanding of the outer radiation belt dynamics in terms of acceleration and loss effects. On the other side, the radiation belt researchers have long been trying to model the outer belt variations (See a review by Shprits et al. 2008). A simple model is based on the radial diffusion of electrons across drift shells over time scales of hours-to-days after being transported from the plasma sheet. However, a comparison with observations indicated that the radial diffusion alone cannot fully explain the observed flux distribution in the outer belt (Miyoshi et al. 2003). It became soon evident that local acceleration effect needs to be taken into account. Presently existing physical models of the radiation belts solve a fully three dimensional, even four dimensional equation of diffusion and transport (e.g., Fok et al. 2008, Shprits et al. 2009). These models include the local diffusion in energy (or momentum) and pitch angle, radial diffusion across drift shells, and the transport from the plasma sheet. Determination of the diffusion coefficients and transport effect for each responsible process is critical and remains a major research topic.

In the present paper, we adopt a strategy to model the outer belt electron distribution based on the radial diffusion equation with observationally determined specifications of a few critical factors. We use observationally determined functional forms for the outer edge boundary conditions and plasmapause locations. Most importantly, we modify the radial diffusion equation by incorporating chorus effect as a source term in an empirical way. We present a comparison between the results with and without the chorus effect and demonstrate the effectiveness of our simple model. The main purpose of this paper is to give a description of the essence of this new model.

2. PHYSICAL STRUCTURE OF THE MODEL

Our model is based on the one-dimensional radial diffusion equation that is modified by inclusion of a term representing the chorus effect, $cB_w f$, as follows.

$$\frac{\partial f}{\partial t} = L_*^2 \frac{\partial f}{\partial L_*}\left(\frac{D_{L_*L_*}}{L_*^2}\frac{\partial f}{\partial L_*}\right) + \left(cB_w - \frac{1}{\tau}\right)f \qquad (1)$$

where f is the phase space density (PSD), $D_{L^*L^*}$ the radial diffusion coefficient, c a calibration factor, B_w the chorus wave intensity, and τ the atmospheric loss time scale. The second bracket term therefore reflects both the chorus-provided source effect (cB_w) and the loss effect by atmospheric precipitation ($1/\tau$) in a simplified way (Tu et al. 2009). Other than the initial condition which is rather flexible to prescribe and does not affect the long term solution seriously, the solution of this equation depends on several major factors. We describe how they are treated in our model below.

First, for the diffusion coefficient $D_{L^*L^*}$, we use the K_p-dependent formula given by Brautigam and& Albert (2000) below.

$$D_{L^*L^*}(K_p, L^*) = 10^{(0.506K_p - 9.325)} L_*^{10} / day \qquad (2)$$

This reflects a temporal dependence in an implicit way via time-varying K_p, which can be predicted by a separate program whenever necessary.

Second, formally Equation (1) is an initial value and boundary condition problem. In particular, the radiation belt electron fluxes are strongly affected by the energy spectrum of the electron flux at the outer boundary. If local acceleration and loss effects are ignored, the radiation belt structure is determined entirely by radial diffusion process which is subject to the boundary condition. Thus specifying the outer boundary condition in a precise way is critical. To set the energy spectrum of the electron flux at the outer boundary of the belt, we use the functional forms that we have recently determined using the observations of energetic electrons by solid state telescope on THEMIS (Shin & Lee 2013). In these functions, the boundary fluxes of electrons at various energies (from 30 keV up to 719 keV) at r = 7-8 R_E on the nightside are expressed in terms of past solar wind speed and density. The details of the results are reported in Shin & Lee (2013) – See Table 2 and Fig. 8 in Shin & Lee (2013). An alternative option that we can choose for description of the boundary conditions is to use the energetic electron fluxes measured by GOES 13 or 15 satellites on geosynchronous orbit. We have recently developed a separate neural network-based scheme to predict electron fluxes at geosynchronous orbit by up to 24 hours -- See Ling et al. (2010) for an example of an application of the

neural network technique to geosynchronous electron flux data. This can be used to set the outer boundary conditions as well, but a drawback is that the differential fluxes of electrons are obtained only for 40 keV to 475 keV and one needs an extrapolation to higher energy. Our empirical specification of the outer boundary condition implicitly takes into account the effects due to the drift loss and transport from the plasma sheet.

Third, it is well known that the atmospheric loss time scale τ differs between the regions inside and outside the plasmasphere due to different scattering mechanisms. Therefore, for example, Shprits et al. (2005) set it to be 10 days inside the plasmasphere and scaled it by $3/K_p$ outside the plasmasphere for 0.95 MeV electrons. For our model, we take 10 days inside the plasmasphere and $4/K_p$ outside the plasmasphere, which we find works better, but this can be easily modified whenever necessary. Therefore, a precise knowledge of the plasmapause locations is critical (We stress that the plasmapause location is distinguished from the inner boundary of the simulation domain for which we take L*=2). Specifically, in our model, the plasmapause location is set by an empirical formula that we have recently developed using the THEMIS observations of four years from July 2007 (Cho JH et al., New empirical models of the plasmapause locations identified using THEMIS observations during the ascending phase of solar cycle 24, Manuscript submitted to JGR, 2014). The readers are referred to Angelopoulos (2008) for the THEMIS mission. The formula is a function of past solar wind variables and geomagnetic indices and works better than the previously known functions (Carpenter & Anderson 1992, O'Brien & Moldwin 2003, Larsen et al. 2007).

Fourth, to specify the chorus term which is the most important part in the equation, we first determine the global distribution of chorus wave intensity. We use the THEMIS satellite observations for the interval of about 4 year period from July 2007 through July 2012 excluding the year 2009 when the solar wind conditions and the magnetospheric activities were unusually weak (Lee et al. 2013). Specifically we use the filter bank data of Search Coil Magnetometer (SCM) onboard the THEMIS satellites (Roux et al. 2008). Our method to identify chorus is basically the same as in the previous work by Li et al. (2010). Specifically, we use the data at top three frequency ranges (1390-4000 Hz, 320-904 Hz, 80-227 Hz) out of the six bands of the filter bank data (Cully et al. 2008). Events with the known noise level of 4 pT or less are excluded. We assume that L = 5 is approximately the inner most boundary where the highest frequency band of the filter bank data can cover the typical chorus frequency range (0.1-0.8) f_{ce}. We collect the chorus events when the satellites were located within L = 5 to 10 as long as the satellites were outside the plasmasphere and not inside the magnetosheath. Also, we limit the satellite position to |magnetic latitude| ≤ 25°.

Li et al. (2010) report the global distribution of the chorus amplitude for a similar data set, and we obtain similar results (see Fig. 2 in this paper). Thus we do not repeat to present this in this paper. The main advance in our work is that we have developed a prediction model for a global distribution of chorus intensity. Our chorus model is capable of predicting the chorus intensity by 30 minutes using the z-component of the interplanetary magnetic field and the geomagnetic index AE. The prediction can even be made separately for the near equator region (|magnetic latitude| ≤ 10°) and for the region away from the equator (10° < |magnetic latitude| ≤ 25°). The details of this chorus prediction model will be reported elsewhere (Kim JH et al., A prediction model for the global distribution of whistler chorus waves including latitudinal dependence, Manuscript submitted to JGR 2014). The present version of our radiation belt model does not fully make use of this sophisticated function of the chorus prediction model. Rather our strategy for the present radiation belt model is to employ a simplified version of the chorus model that can be easily incorporated into the diffusion Equation (1).

Specifically, we first obtain the magnetic local time (MLT)–averaged, but L-dependent, chorus amplitude. Fig. 1 shows the obtained profiles in L of the root mean square (RMS) chorus amplitudes averaged over MLT for each 0.1 L bin. The results in Fig. 1 are divided by three AE levels. The red lines are fit functions of 7th order polynomials in L, $B_w = \sum_{i=0}^{7} a_i L^i$, the coefficients of which are summarized in Table 1. Then, we try to express the L-dependent profile of chorus amplitude in terms of the *Roederer*'s drift shell parameter L^* (Roederer 1970). This is necessary since the diffusion Equation (1) that we solve is based on L^* rather than the McIlwain's L. The relationship between L and L^* is in general nontrivial to obtain, but an

Table 1. Coefficients of fit functions for chorus intensity.

	AE<100	100≤AE≤300	300<AE
a_0	-47586.41	-108216.61	-142245.22
a_1	46467.79	107339.79	143642.56
a_2	-19211.83	-45124.36	-61405.46
a_3	4360.77	10424.19	14406.27
a_4	-587.09	-1429.59	-2003.70
a_5	46.90	116.44	165.28
a_6	-2.06	-5.22	-7.49
a_7	0.04	0.10	0.14

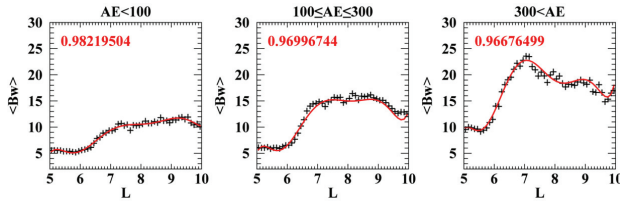

Fig. 1. MLT-averaged chorus intensities as a function of L for three activity levels. The red lines in each panel refer to 7th order polynomial fit curves. The numbers inside the panels are a measure of goodness of the fits, 1 implying a perfect fit.

analytic form can be derived for an analytic magnetospheric field model. Following the suggestion by Su et al. (2011), we use the Dst-dependent Hilmer-Voigt symmetric geomagnetic field model (Hilmer and & Voigt 1995). The derived relationship between L and L^* is as follows (Su et al. 2011).

$$\frac{1}{L_*} = \frac{1}{L} - 4\frac{B_+}{B_o}\frac{r_+^3 L^2}{\left(L^2 + 4r_+^2\right)^{3/2}} - 4\frac{B_-}{B_o}\frac{r_-^3 L^2}{\left(L^2 + 4r_-^2\right)^{3/2}} \quad (3)$$

where B_0 = 31200 nT, and B_+, B_-, r_+, and r_- are Dst-dependent parameters (See Hilmer and & Voigt (1995) for details). Then the observed chorus intensity in Fig. 1 is converted as a function of L^* using the relation (3).

Last, we determine the calibration factor c of the chorus term by minimizing the difference between the predictions and observations separately for three AE levels: c = 0.08 for AE < 100 nT, and c = 0.1 for both 100 ≤ AE ≤ 300 and AE > 300 nT.

3. EXAMPE OF MODEL RUNS

Fig. 2a shows the observationally identified plasmapause locations L_{pp} (black) overlaid on the 719 keV electron flux for the 4 year interval. L_{pp} approximately coincides with the inner edge of the energetic electron flux throughout the whole interval. However, a closer examination indicates that when the radiation belt is strong, the inner edge of the belt temporarily penetrates into the plasmasphere that shrinks itself, as noted previously (e.g., Li et al. 2006). An outstanding feature in the studied interval is that the plasmasphere expanded greatly as far as geosynchronous altitude or even beyond when the outer belt became nearly lost a few times, each for a long term, in 2009 (Lee et al. 2013). Fig. 2b shows a comparison between the observationally identified plasmapause locations (black, the same curve as in Fig. 2a) and our plasmapause location model result (magenta) for the

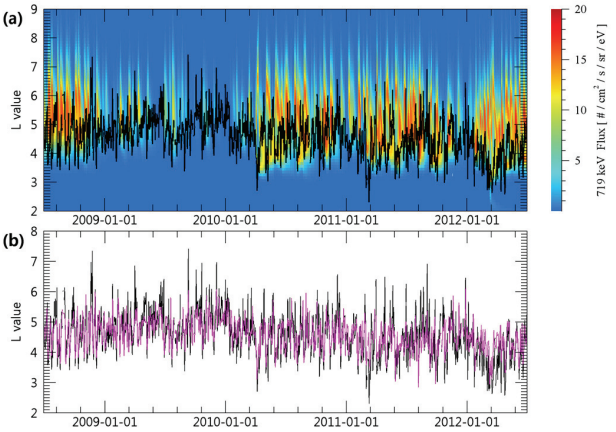

Fig. 2. (a) Daily averaged L_{pp} (black line) superposed on the 719 keV electron flux measured on the THEMIS SST instrument. (b) Daily averaged observed L_{pp} (black line) and our model L_{pp} (magenta) as a function of solar wind speed, IMF B_z, and AE index.

same 4 year interval for which the model was constructed. The agreement between the observation and model is estimated by a parameter that we call the prediction efficiency defined below.

$$PE = 1 - \frac{\sum_{i=1}^{n}\left(d_i - p_i\right)^2}{\sum_{i=1}^{n}\left(d_i - \langle d\rangle\right)^2} \quad (4)$$

where d_i and p_i are the observed and model data points, respectively, and <d> is the mean of the n number of the observed data point, i.e., all d_i. PE = 0 means that the model results are as good as the averaged observation data, and PE = 1 means a perfect modeling (Tu et al. 2009). In Fig. 2b where daily averaged values are compared, PE is 0.519.

In Fig. 3 we present the results of application of (1) to a new interval. The panels (a) and (b) in Fig. 3 show the predicted fluxes of 1 MeV electrons with and without the chorus term, respectively. The difference between the two simulation results in Fig. 3 is clear enough to identify that the flux enhancement at the central region of the outer belt is more pronounced when the chorus effect is included. Elsewhere the chorus effect appears to make no significant difference. Also there is no major difference in the inner boundary position of the outer belt between the two simulations. We estimate the prediction efficiency of each model result with the observations made by the Van Allen Probes. Table 2 shows the results for selected L^* values. It indicates that PE is larger at all L^* values for the model with the chorus effect than for the model without it. In fact, PE for the model without the chorus effect is below zero at all L^* implying that its performance is worse

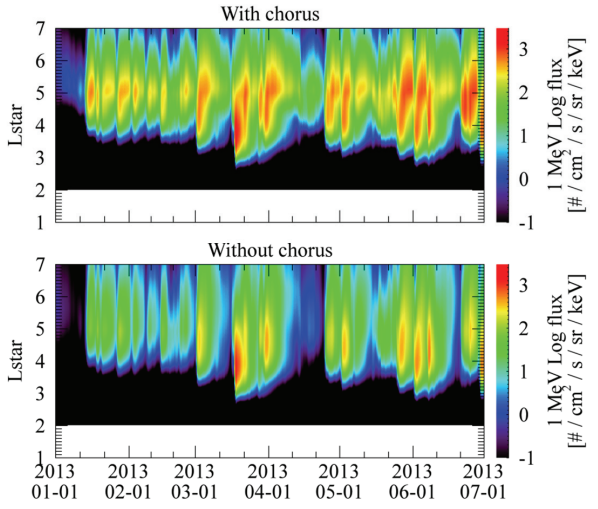

Fig. 3. Comparison of electron fluxes obtained from the diffusion equations with and without the chorus acceleration effect.

Table 2. Comparison of prediction efficiency between the diffusion results with and without chorus.

	L^*=5	L^*=5.5	L^*=6
With Chorus	-0.35	0.5	0.7
Without Chorus	-1.5	-1.3	-0.15

than predicting an average trend of the observation. Therefore, the simulation result with the inclusion of chorus term agrees better with the actual observations. However, the prediction efficiency becomes lower at lower L^* even for the model with the chorus effect, requiring an improvement of the model performance in future.

4. SUMMARY AND FUTURE WORKS

In this paper, we described the physical formalism of the outer radiation belt model that we have recently developed at Chungbuk National University. The model is based on the simple, mathematically one-dimensional, but physically higher dimensional, equation of diffusion. We have determined three main factors observationally that affect the solution of the diffusion equation. They are the boundary condition at the outer edge of the outer belt, the plasmapause location, and the chorus acceleration effect. The developed model captures the flux enhancement at the central region of the outer radiation belt to some reasonable degree. While, for a more rigorous treatment of diffusion physics, one has to rely on a more "expensive" three dimensional diffusion equation (e.g., Shprits et al. 2009), our simplified model is more suitable for space weather forecast purpose. Improvement of the effects included here and further addition of other effects will further enhance the accuracy of the model.

We plan to improve our model in the following aspects. First, we will develop a better scheme for the L to L^* conversion since the L to L^* conversion inevitably suffers from errors particularly at a larger radial distance. Second, we will incorporate the effects by other waves such as electromagnetic ion cyclotron waves and plasmaspheric hiss waves to improve the associated precipitation effect. Lastly, we will use this physical model to develop a data assimilation model along with available observations.

ACKNOWLEDGEMENTS

This work at Chungbuk National University was supported by a NSL grant (NRF-2011-0030742) from the National Research Foundation of Korea. We acknowledge NASA contract NAS5-02099 and V. Angelopoulos for use of data from the THEMIS Mission. Our model presented here is an extension of the original version of the one-dimensional radial diffusion code written by Kyung-Chan Kim.

REFERENCES

Angelopoulos V, The THEMIS mission, SSRv 141, 5-34 (2008). http://dx.doi.org/10.1007/s11214-008-9336-1

Baker D, Kanekal SG, Hoxie VC, Henderson MG, Li X, et al., A long-lived relativistic electron storage ring embedded in earth's outer Van Allen Belt, Science 340, 186-190 (2013). http://dx.doi.org/10.1126/science.1233518

Brautigam DH, Albert J, Radial diffusion analysis of outer radiation belt electrons during the October 9, 1990, magnetic storm, JGR 105, 291-310 (2000). http://dx.doi.org/10.1029/1999JA900344

Carpenter DL, Anderson RR, An ISEE/whistler model of equatorial electron density in the magnetosphere, JGR 97, 1097-1108 (1992). http://dx.doi.org/10.1029/91JA01548

Cully CM, Ergun RE, Steevens K, Nammari A, Westfall J, The THEMIS digital field board, SSRv 141, 343-355 (2008). http://dx.doi.org/10.1007/s11214-008-9417-1

Fok MC, Horne RB, Meredith NP, Glauert SA, Radiation Belt Environment model: Application to space weather nowcasting, JGR 113, A03S08 (2008). http://dx.doi.org/10.1029/2007JA012558

Horne RB, Thorne RM, Relativistic electron acceleration and precipitation during resonant interactions with whistler-mode chorus, GRL 30, 34-1 (2003). http://

dx.doi.org/10.1029/2003GL016973

Hwang J, Lee DY, Kim KC, Shin DK, Kim JH, et al., Significant loss of energetic electrons at the heart of the outer radiation belt during weak magnetic storms, JGR 118, 4221-4236 (2013). http://dx.doi.org/10.1002/jgra.50410

Hilmer RV, Voigt G, A magnetospheric magnetic field model with flexible current systems driven by independent physical parameters, JGR 100, 5613-5626 (1995). http://dx.doi.org/10.1029/94JA03139

Kim KC, Lee DY, Kim HJ, Lyons LR, Lee ES, et al., Numerical calculations of relativistic electron drift loss effect, JGR 113, A09212 (2008). http://dx.doi.org/10.1029/2007JA013011

Kim KC, Lee DY, Kim HJ, Lee ES, Choi CR, Numerical estimates of drift loss and Dst effect for outer radiation belt relativistic electrons with arbitrary pitch angle, JGR 115, A03208 (2010). http://dx.doi.org/10.1029/2009JA014523

Kim KC, Shprits Y, Subbotin D, Ni B, Understanding the dynamic evolution of the relativistic electron slot region including radial and pitch angle diffusion, JGR 116, A10214 (2011). http://dx.doi.org/10.1029/2011JA016684

Lam MM, Horne RB, Meredith NP, Glauert SA, Moffat-Griffin T, et al., Origin of energetic electron precipitation > 30 keV into the atmosphere, JGR 115, A00F08 (2010). http://dx.doi.org/10.1029/2009JA014619

Larsen BA, Klumpar DM, Gurgiolo C, Correlation between plasmapause position and solar wind variables, JASTP 69, 334-340 (2007). http://dx.doi.org/10.1016/j.jastp.2006.06.017

Lee DY, Shin DK, Kim JH, Cho JH, Kim KC, et al., Long-term loss and re-formation of the outer radiation belt, JGR 118, 3297-3313 (2013). http://dx.doi.org/10.1002/jgra.50357

Lee JJ, Parks GK, Min KW, McCarthy MP, Lee ES, et al., Relativistic electron dropouts by pitch angle scattering in the geomagnetic tail, Ann. Geophys. 24, 3151–3159 (2006). http://dx.doi.org/10.5194/angeo-24-3151-2006

Li W, Thorne RM, Nishimura Y, Bortnik J, Angelopoulos V, et al., THEMIS analysis of observed equatorial electron distributions responsible for the chorus excitation, JGR 115, A00F11 (2010). http://dx.doi.org/10.1029/2009JA014845

Li X, Roth I, Temerin M, Wygant J, Hudson MK, et al., Simulation of the prompt energization and transport of radiation particles during the March 24, 2991 SSC, GRL 20, 2423-2426 (1993). http://dx.doi.org/10.1029/93GL02701

Li X, Baker DN, O'Brien TP, Xie L, Zong QG, Correlation between the inner edge of outer radiation belt electrons and the inner most plasmapause location, GRL 33, L14107 (2006). http://dx.doi.org/10.1029/2006GL026294

Li X, Roth I, Temerin M, Baker DN, Reeves GD, Behavior of MeV electrons at geosynchronous orbit during last two solar cycles, JGR 116, A11207 (2011). http://dx.doi.org/10.1029/2011JA016934

Ling AG, Ginet GP, Hilmer RV, Perry KL, A neural network-based geosynchronous relativistic electron flux forecasting model, Space Weather 8, S09003 (2010). http://dx.doi.org/10.1029/2010SW000576

Meredith NP, Horne RB, Johnstone AD, Anderson RR, The temporal evolution of electron distributions and associated wave activity following substorm injections in the inner magnetosphere, JGR 105, 12907-12917 (2000). http://dx.doi.org/10.1029/2000JA900010

Miyoshi Y, Morioka A, Obara T, Misawa H, Nagai T, et al., Rebuilding process of the outer radiation belt during the 3 November 1993 magnetic storm: NOAA and Exos-D observations, JGR 108, SMP 3-1 (2003). http://dx.doi.org/10.1029/2001JA007542

O'Brien TP, Moldwin MB, Empirical plasmapause models from magnetic indices, GRL 30, 1-1 (2003). http://dx.doi.org/10.1029/2002GL016007

Onsager TG, Rostoker G, Kim HJ, Reeves GD, Obara T, et al., Radiation belt electron flux dropouts: Local time, radial and particle-energy dependence, JGR 107, SMP 21-1 (2002). http://dx.doi.org/10.1029/2001JA000187

Reeves GD, McAdams KL, Friedel RHW, Acceleration and loss of relativistic electrons during geomagnetic storms, GRL 30, 36-1 (2003). http://dx.doi.org/10.1029/2002GL016513

Roederer JG, Dynamics of geomagnetically trapped radiation (Springer, Berlin 1970).

Roux A, Le Contel O, Coillot C, Bouabdellah A, de la Porte B, Alison D, Ruocco S, Vassal MC, The search coil magnetometer for THEMIS, SSRv 141, 265-275 (2008). http://dx.doi.org/10.1007/s11214-008-9455-8

Shin DK, Lee DY, Determining radial boundary conditions of outer radiation belt electrons using THEMIS observations, JGR 118, 2888-2896 (2013). http://dx.doi.org/10.1002/jgra.50334

Shprits YY, Thorne RM, Reeves GD, Friedel R, Radial diffusion modeling with empirical lifetimes: comparison with CRRES observations, Ann. Geophys. 23, 1467-1471 (2005). http://dx.doi.org/10.5194/angeo-23-1467-2005

Shprits YY, Subbotin DA, Meredith NP, Elkington SR, Review of modeling of losses and sources of relativistic electrons in the outer radiation belt II: Local acceleration and loss, JASTP 70, 1694-1713 (2008). http://dx.doi.org/10.1016/j.jastp.2008.06.014

Shprits YY, Subbotin DA, Ni B, Evolution of electron fluxes in the outer radiation belt computed with the VERB code, JGR 114, A11209 (2009). http://dx.doi.

org/10.1029/2008JA013784

Summers D, Ni B, Meredith NP, Timescales for radiation belt electron acceleration and loss due to resonant wave-particle interactions: 2. Evaluation for VLF chorus, ELF hiss, and electromagnetic ion cyclotron waves, JGR 112, A04207 (2007). http://dx.doi.org/10.1029/2006JA011993

Su Z, Xiao F, Zheng H, Wang S, Radiation belt electron dynamics driven by adiabatic transport, radial diffusion, and wave-particle interactions, JGR 116, A04205 (2011). http://dx.doi.org/10.1029/2010JA016228

Tu W, Li X, Chen Y, Reeves GD, Temerin M, Storm-dependent radiation belt electron dynamics, JGR 114, A02217 (2009). http://dx.doi.org/10.1029/2008JA013480

Turner DL, Shprits Y, Hartinger M, Angelopoulos V, Explaining sudden losses of outer radiation belt electrons during geomagnetic storms, Nature Physics 8, 208-212 (2012). http://dx.doi.org/10.1038/NPHYS2185